Frontiers in Bioscience Landmark

Front. Biosci. (Landmark Ed) **2023**; 28(1): 17
https://doi.org/10.31083/j.fbl2801017

Original Research

KMT2D Regulates the *NCOA6/THRB* Signal Axis through Epigenetic Modification to Promote the Migration and Invasion of Papillary Thyroid Cancer

Rui Wang[1], Yibo He[1], Yi Wang[1], Shangnao Xie[1,*]

[1]Surgical Oncology, Hangzhou Cancer Hospital, 310002 Hangzhou, Zhejiang, China
*Correspondence: xieshangnao@126.com (Shangnao Xie)
Academic Editor: Natascia Tiso
Submitted: 25 August 2022 Revised: 25 November 2022 Accepted: 6 December 2022 Published: 18 January 2023

Abstract

Background: The histone lysine methyltransferase Histone-lysine N-methytransferase 2D (*KMT2D*) is a common mutated gene in a variety of cancers, including papillary thyroid cancer (PTC). However, the mechanism of *KMT2D* on the progression of PTC remains unclear. **Methods**: In this study, quantitative real-time polymerase chain reaction (qRT-PCR) and Western blotting were used to evaluate *KMT2D* expression between human normal cell (Nthy-ori 3-1) and PTC cells (TPC1, IHH-4 and BCPAP). Proliferation, migration and invasion of TPC1, IHH-4 and BCPAP were assessed by Cell Counting Kit-8 (CCK-8), Wound-healing assay and Transwell assay. The mechanism of *KMT2D* on thyroid papillary cancer was explored with Chromatin immunoprecipitation assay (ChIP), qRT-PCR and Western blotting. **Results**: The expression of *KMT2D* in PTC cells was significantly increased. Downregulation of *KMT2D* significantly decreased the proliferation, migration and invasion of PTC cells, which was correlated with decreased expression levels of *H3K4me2, H3K9me2, NCOA6* and *THRB*. Meanwhile, ChIP assay demonstrated that *KMT2D* was associated with *NCOA6*. **Conclusions**: Study have shown that the downregulation of *KMT2D* reduces proliferation, migration and invasion of thyroid papillary carcinoma cells through epigenetic modification of *NCOA6/THRB* signal axis. These results provide a new insight into the role of *KMT2D* in migration and invasion of PTC.

Keywords: papillary thyroid cancer; *KMT2D*; epigenetic modification; migration; invasion

1. Introduction

Thyroid cancer (TC) is the most common malignant disease of endocrine system, and its incidence has been on the rise in recent years. In 2019, there were 233,846 new cases of thyroid cancer and 45,575 deaths from the disease worldwide [1]. China has the highest number of thyroid cancer cases and deaths in the world. Papillary thyroid cancer (PTC) accounts for approximately 90% of all thyroid cancers, and the increased incidence and mortality of PTC leads to an actual increase in all TC cases [2,3]. The incidence of PTC increases with age, with more women than men [4]. Surgery is usually the first line of treatment for PTC. However, the prevalence of PTC remains a concern, as the recurrence rate of PTC is close to 30% and the cause-specific mortality rate over a 30-year period is 8.6% [5]. Therefore, it is an urgent and necessary task to find diagnostic markers and new therapeutic targets for PTC recurrence and metastasis.

The pathogenesis and progression of PTC has been reported to be associated with genetic and epigenetic alterations, including driver point mutations in *BRAF* and *RAS*, the diverse gene fusion (*RET/PTC, ETV6-NTRK3*) and miR146b, miR21, etc. [6,7]. The cancer genome atlas project identified 299 genes and 24 pathways that drive tumor progression, including 12 genes involved in histones, histone methylation and demethylation [8]. Our previous studies found that thyroid cancer could induce Histone-lysine N-methytransferase 2D (*KMT2D*) to inhibit apoptosis by regulating *H3K4* site and *NCOA1/6* in the protein function and protein network analysis (**Supplementary Fig. 1**). In TC patients, *KMT2D* mutation status is associated with shorter disease-specific survival. Thanyawat *et al*. [9] also found that epigenetic modifications of *KMT2D* are involved in the malignant progression of TC. *KMT2D* is a histone methyltransferase that stimulates tumor growth and triggers metastasis. *KMT2D* is located on chromosome 12q13.12 and is widely expressed in adult tissues. It is reported that *KMT2D* plays a role in binding enhancer regions and maintaining global *H3K4me1/2* levels. *H3K4me2* and *H3K9me2* are strongly associated with gene transcription. *H3K4me2* is found in a wider range of promoters, enhancers and long-range regulatory elements. *H3K9me2* presents chromatin extensively and is enriched in a number of tightly-controlled signaling and cell-type specific pathways. In addition, *KMT2D* is one of the most commonly mutated genes in many different types of cancer. In breast cancer, the PI3K pathway regulates ER-dependent transcription through the epigenetic regulator *KMT2D* [10]. Ming *et al*. [11] indicated that *KMT2D* regulates *H3K4* methylation and participates in the pathology of ovarian cancer. These studies suggest that *KMT2D* may play an

Table 1. Primer sequence.

Gene	Amplicon lengths	Forward primer	Reverse primer
KMT2D	793	GACACAACAACACGATGCTCC	ACGTGACCTCTATGCAACCC
NCOA6	167	AAAACGTGCCCAATTTGTTACAC	GAGAATCCCTAAATCCCGAAGC
THRB	86	TGGGACAAACCGAAGCACTG	TGGCTCTTCCTATGTAGGCAG
GAPDH	119	TGTGGGCATCAATGGATTTGG	ACACCATGTATTCCGGGTCAAT

important role in PTC.

Consequently, we focused on the histone methyltransferase *KMT2D* to explore the specific mechanism of PTC carcinogenesis and invasion. In this study, we analyzed *KMT2D* expression levels in different thyroid cancer cell lines and evaluated *KMT2D*-mediated epigenetic modification on the progression of PTC. And, we proposed that inhibitors targeting the *KMT2D* gene may be used for the treatment of PTC.

2. Materials and Methods

2.1 Cell Culture and Reagents

TPC1 (iCell-h309), IHH-4 and BCPAP (iCell-h022) cells were purchased from iCell Bioscience Inc (Shanghai, China). All thyroid papillary carcinoma cell lines were cultured in Dulbecco's modified Eagle's Medium (DMEM, Hyclone, Logan, Utah, USA) supplemented with 10% fetal bovine serum (FBS, ZhejingTianhang Biotechnology Co. Ltd, Hangzhou, China). A human normal cell line Nthy-ori 3-1 was required from iCell Bioscience Inc and cultured in RPMI medium 1640 with 10% FBS. All cells were maintained in a humidified atmosphere at 5% CO_2 and 37 °C.

2.2 RNA Interference and Transfection

TPC1, IHH-4 and BCPAP cells were seeded into 6-well plates, and transfected with two siRNA targeting *KMT2D* or negative control (NC) using lipofectamine 2000 (Thermo Fisher Scientific, Waltham, MA, USA). The efficacy of RNA interference in thyroid papillary carcinoma cells was assessed by qRT-PCR. Compared with sh-NC group, the mRNA level of *KMT2D* was significantly decreased in si-*KMT2D* (1) and si-*KMT2D* (2) group (**Supplementary Fig. 2**).

2.3 qRT-PCR

RNA was isolated from Nthy-ori3-1, TPC, IHH-4 and BCPAP cells with Trizol (Sangon Biotech, Shanghai, China). The total RNA was reverse transcribed into cDNA at the following condition: 95 °C, 10 min; 95 °C, 15 s; 60 °C, 60 s; 40 cycles. The mRNA expression was quantified by the SYBR Premix Ex TaqII (Takara, Shiga, Japan) and normalized by Glyceraldehyde-3-phosphate dehydrogenase (GAPDH). The primers were listed in Table 1.

2.4 Western Blotting

The cells were trypsinized, harvested and lysed in Radio-Immunoprecipitation Assay (RIPA) buffer containing phenylmethylsulfonyl fluoride (PMSF) (Beyotime, Shanghai, China) and protease inhibitor (CWBIO, Beijing, China). The concentration of total protein was measured by the BCA Protein Assay Kit (Beijing Solarbio Science & Technology Co., Ltd, Beijing, China). After loading samples, proteins were migrated by Sodium dodecyl-sulfate polyacrylamide gel electrophoresis (SDS PAGE) and transferred to polyvinylidene fluoride (PVDF) membranes, which were then blocked with non-fat milk for 2 h. The primary antibody was used to incubate membrane overnight at 4 °C. The antibodies were bought from Affinity Biosciences company (KMT2D Antibody: DF9646; H3K4me2 Antibody: AF0589; H3K9me2 Antibody: DF6937; NCOA6 Antibody: DF13176; THRB Antibody: AF0357; H3 Antibody: AF0863; GAPDH Antibody: AF7021). The second antibody was diluted with non-fat milk and incubated membrane for 1.5 h at room temperature. ECL detection kit and ChemiScope 6100 (Clinx Science Instruments Co., Ltd, Shanghai, China) were used to visualize protein bands.

2.5 Chromatin Immunoprecipitation Assay (ChIP)

High-sensitivity ChIP Kit (ab185913, abcam, Cambridge, UK) was used in this study. We assessed the association between KMT2D and NCOA6. The protocol was as follow: (1) Formaldehyde cross-linking and ultrasonic crushing of cells: the cells were removed, formaldehyde was added to make the final concentration of formaldehyde 1%, and the cells were incubated at 37 °C for 10 min. The cross-linking was terminated, the medium was sucked up, and the cells were washed twice with cold Polybutylene Succinate (PBS). The cells were collected in a 15 mL centrifuge tube with a cell scraper. After pre-cooling, the cells were collected by centrifugation, and the supernatant was poured out. (2) Impurity removal and antibody feeding: after ultrasonic crushing, centrifuge to remove insoluble substances; A 900µL dilution Buffer and 20 µL of 50×polyisocyanopeptide (PIC) are added to 100 µL of the ultrasonic fragmentation product. Then 60 µL of Protein A arose/Salmon Sperm DNA was added. Toss and mix at 4 °C for 1 h; After 1 h, the samples were left at 4 °C for 10 min to precipitate and centrifuged at 700 rpm for 1 min. Take the supernatant. 20 µL of each will be reserved as input. Antibody was added to one tube and no antibody was added to the other overnight at 4 °C. (3) Test the effect of ultrasonic crushing: Take 100 µL of the product after ultrasonic crushing, add 4 µL 5M NaCl, and treat

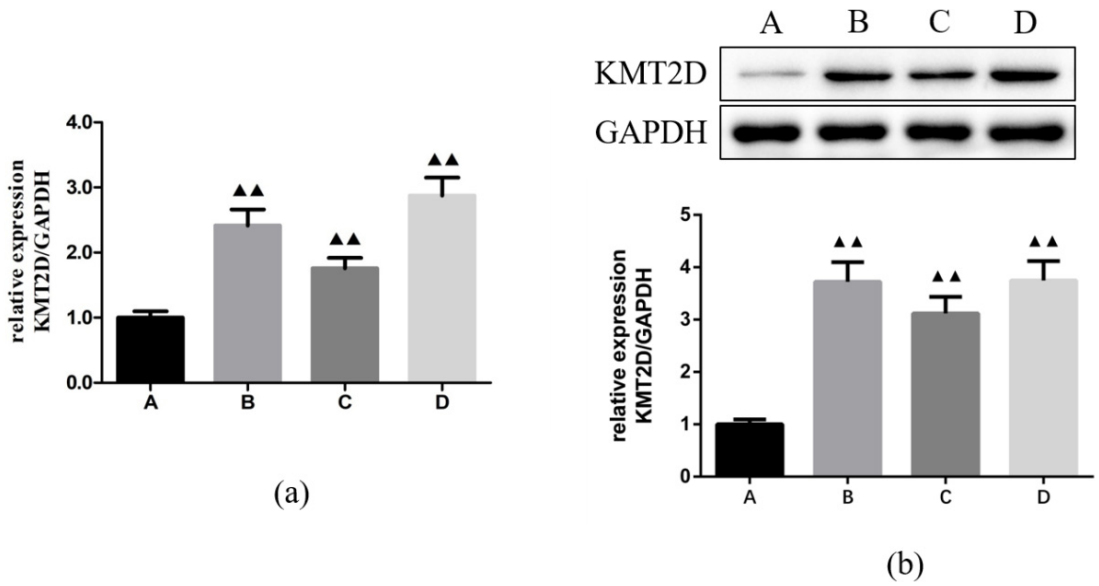

Fig. 1. The mRNA and protein expressions of *KMT2D* in Nthy-ori3-1, TPC, IHH-4 and BCPAP cells. (a) qRT-PCR analysis. (b) Western blotting analysis. A: Nthy-ori3-1 cell; B: TPC cell; C: IHH-4 cell; D: BCPAP cell. $^{▲▲}p < 0.01$.

it at 65 °C for 2 h to uncross-link. Half was extracted with phenol/chloroform. Ultrasonic effect was detected by electrophoresis. (4) Precipitation and cleaning of immune complexes: After overnight incubation, 60 µL Protein A Agarose/Salmon Sperm DNA was added to each tube at 4 °C for 2 h; After 10min, the supernatant was removed by centrifugation. Wash the precipitated complex. Then, 20 µL NaCl was added to elution. (5) Recovery of DNA samples: After unlinking overnight, 1 µL RNaseA was added and incubated at 37 °C for 1 h. 10 µL EDTA, 20 µL Tris HCl (pH 6.5), 2 µL 10 mg/mL proteinase K was added for 2 h, subsequently. The final sample was dissolved in 100 µL H_2O. (6) The bound target DNA fraction was amplified by PCR.

2.6 Cell Counting Kit-8 (CCK-8)

Cells were seeded in a 96-well plate for 24 h, and 10 μL CCK-8was added. The availability of cells was detected by CCK-8 kit (MedChemExpress, New Jersey, USA) at 0 h, 24 h, 48 h and 72 h after siRNA transfection. The results were determined by microplate reader (Molecular Devices, Silicon Valley, USA) at 450 nm.

2.7 Wound-Healing Assay

Cells were resuspended in serum-free medium, added to a six-well plate (5×10^5 cells/well) overnight. The wounds were made using a 10 μL pipette tip, cell debris was removed by washing with PBS for three times. Wound healing was observed under an inverted microscope at 0 h and 12 h. Cells migration was assessed by ImageJ v1.8.0 software (National Institutes of Health, New York, USA).

2.8 Transwell Assay

Cells were added into the upper chambers of 24-well transwell chambers (Corning, New York, USA) with or without BD Matrigel (invasion assay and migration assay). After 24 h of incubation, cells on the surface of upper chamber were removed with cotton swabs. The invaded/migrated cells on the lower surface were fixed with 4% paraformaldehyde and stained with 0.1% crystal violet. Cells were imaged and counted in five random fields.

2.9 Statistical Analysis

Statistical analysis was performed with SPSS 18.0 software (IBM Corp., Chicago, IL, USA) and GraphPad Prism 8 software (GraphPad Software Inc., San Diego, CA, USA). Each experiment was repeated three times. Differences between two groups were made using Independent sample *T* test or Kruskal-Wallis H Test. All data were expressed as the means $\pm$ standard deviations, $p < 0.05$ was considered statistically significant.

3. Results

3.1 Overexpression of KMT2D in Thyroid Papillary Carcinoma Cells

We compared the expression of *KMT2D* in thyroid papillary carcinoma cell lines and normal thyroid follicular cell line by qRT-PCR and Western blotting (Fig. 1). The results demonstrated that *KMT2D* mRNA levels were significantly higher in TPC, IHH-4 and BCPAP cells than in Nthy-ori3-1 cell. Western blotting analysis of *KMT2D* protein confirmed the RNA expression data, showing remarkably higher expression in thyroid papillary carcinoma cells than in normal thyroid cell.

3.2 KMT2D Knockdown Inhibits Proliferation, Migration and Invasion of Thyroid Papillary Carcinoma Cells

TPC, IHH-4 and BCPAP cells were transfected with *KMT2D* inhibitors or NC to evaluate the effect of *KMT2D* in thyroid papillary carcinoma cells. CCK-8 assay demonstrated the cell viability in si-*KMT2D* (1) and si-*KMT2D* (2) groups was lower than in si-NC group (Fig. 2a). It indicated that *KMT2D* knockdown suppressed the proliferation of TPC, IHH-4 and BCPAP cells. Then, Wound healing and Transwell assay were used to investigate the role of *KMT2D* in the cell invasion and migration. As shown in Fig. 2b, the migration distances in si-*KMT2D* (1) and si-*KMT2D* (2) groups were less than si-NC group at 12 h after scratch. Similarly, the Transwell assay showed a significantly decrease in the number of migrated cells in si-*KMT2D* group ($p < 0.01$). The number of invaded cells in *KMT2D* gene silence group decreased remarkably compared with si-NC group ($p < 0.01$, Fig. 2c). These results indicated that *KMT2D* promotes the proliferation, migration and invasion of thyroid papillary carcinoma cells.

3.3 The Mechanism of KMT2D on Papillary Thyroid Cancer

ChIP assay showed that *KMT2D* is associated with *NCOA6* in TPC, IHH-4 and BCPAP cells (Fig. 3a). Compared with anti-IgG group, the input of *NCOA6* is significantly increased in anti-*KMT2D* group. To understand why *KMT2D* is required for the activities of *NCOA6*, we examined the levels of *H3K4me2* and *H3K9me2*, which are closely correlated with active enhancers and promoters. Western blotting showed that silencing *KMT2D* (si-*KMT2D*) was significantly upregulated *H3K4me2* and *H3K9me2* at protein levels (Fig. 3c). In addition, western blotting and qRT-PCR analysis were used to explore the association of *KMT2D* and *NCOA6*. As shown in Fig. 3b,c, *KMT2D* knock out markedly decreased the expression of *NCOA6* and *THRB* compared with si-NC group. These results demonstrated that *KMT2D* regulates the expression of *NCOA6* and *THRB* through demethylation of *H3K4me2* and *H3K9me2* in thyroid papillary carcinoma cells.

4. Discussion

KMT2D plays an important role in tumorigenesis, differentiation, metabolism and inhibition. *KMT2D* mutations are common in various types of cancer, including the brain, lymph nodes, blood, lung, thyroid, intestine, and endometrium [12–14]. The anti- or pro-tumor effects of *KMT2D* are related to cell types. In bladder cancer tissues and cell lines, *KMT2D* is downregulated and its overexpression could significantly alleviate tumor progression [15]. *KMT2D* also exhibits tumor suppressor effects in melanoma and pancreatic cancer cells [16,17]. It may depend on the inhibition of downregulated oncogenes, including *PTEN, P53* and *STAG2* [18]. On the other hand, *KMT2D* is required for the formation of acute myeloid leukemia and is highly expressed in esophageal squamous cell carcinoma, prostate cancer, pancreatic and gastric cancer [15]. In this

Fig. 2. *KMT2D* regulates migration and invasion in TPC, IHH-4 and BCPAP cells. (a) CCK8 assay. (b) Wound healing. (c) Transwell assay. $^{\blacktriangle}p < 0.05$, $^{\blacktriangle\blacktriangle}p < 0.01$.

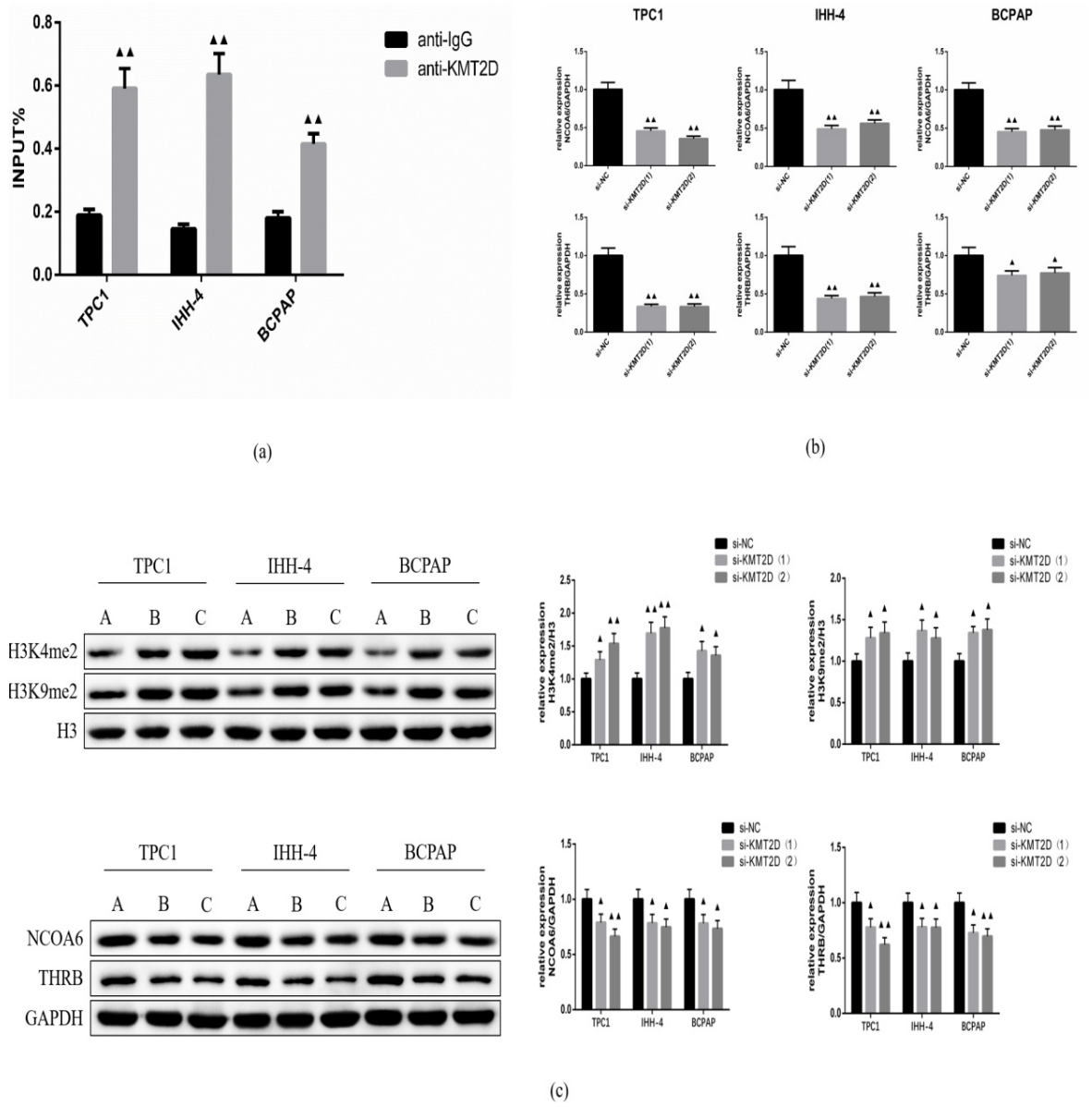

Fig. 3. The mechanism of *KMT2D* on papillary thyroid carcinoma cells. (a) ChIP assay. (b) qRT-PCR analysis. (c) Western blotting analysis. A, si-NC; B, si-*KMT2D* (1); C, si- *KMT2D* (1). $^{\blacktriangle}p < 0.05$, $^{\blacktriangle\blacktriangle}p < 0.01$.

study, we found that *KMT2D* was overexpressed in PTC cell lines by qRT-PCR and Western blotting. It suggests that *KMT2D* may play an important role in the initiation and development of PTC. *KMT2D* deficiency has been associated with cell proliferation and apoptosis in gastric, pancreatic, prostate and colon cancer [19]. Consistent with previous findings, *KMT2D* knockdown inhibited the proliferation, migration and invasion of TPC, IHH-4 and BCPAP cells. It indicated the tumor inhibition of *KMT2D* on PTC.

Then, we studied the underlying mechanism of *KMT2D* mutations on PTC. *KMT2D* mutations lead to defective enhancer regulation and genomic instability during DNA replication and/or transcription [20]. *KMT2D* is associated with *WRAD, NCOA6, PTIP, PA1* and *H3K27* demethylase *UTX* in protein complexes. Cefan *et al*. [21] reported that Pygo2 is involved in the progression of glioma by upregulating the *KMT2D* complex and H3K4me3. Whole exome sequencing showed that there were 6 harmful mutations (*ARID1A, NCOR2, KMT2D, NCOA6, MECP2 a*nd *SUPT6H*) in the epigenetic regulation of colorectal cancer in Chinese patients. Moreover, *KMT2D* and *NCOA6* encode subunits of histone H3K4 methyltransferase protein complexes that act as coactivators of p53 [20]. In this study, ChIP assay confirmed the binding of *KMT2D* and *NCOA6* in PTC cells. Meanwhile, the mRNA and protein levels of *NCOA6* and *THRB* were significantly decreased in si-*KMT2D* thyroid cells, suggesting that *KMT2D* modulates the expression of *NCOA6/THRB* signal axis. In addition, western blotting showed that si-*KMT2D* could upregulate the expression of *H3K4me2* and *H3K9me2* in TPC, IHH-4

and BCPAP cells. The role of *KMT2D* in epigenetic regulation was demonstrated.

In summary, we found that *KMT2D* is markedly upregulated in PTC cells and plays a vital role in the migration and invasion of PTC cells. *KMT2D* knockdown could regulate the expression of *NCOA6, THRB, H3K4me2* and *H3K9me2*. The results indicated that *KMT2D* regulated the *NCOA6/THRB* signaling axis through epigenetic modification, promoting the migration and invasion of PTC.

5. Conclusions

In conclusion, we have identified that *NCOA6/THRB* signal axis as a target of *KMT2D* in PTC cells, which may be regulated by epigenetic modification. It provides new insights into the role of *KMT2D* in the treatment of PTC.

Availability of Data and Materials

All data generated or analyzed during this study are included in this published article.

Author Contributions

RW and YH mainly performed this study, RW wrote the draft, SX supervised this study, YW analyzed data.

Ethics Approval and Consent to Participate

This project was approval by Hangzhou Cancer Hospital ethic commitment. (HZCH-2020-109).

Acknowledgment

We sincerely thank all who participated in this study.

Funding

This study was supported by Hangzhou Science and technology Development plan project (20201231Y031).

Conflict of Interest

The authors declare no conflict of interest.

Supplementary Material

Supplementary material associated with this article can be found, in the online version, at https://doi.org/10.31083/j.fbl2801017.

References

[1] Deng Y, Li H, Wang M, Li N, Tian T, Wu Y, *et al*. Global Burden of Thyroid Cancer from 1990 to 2017. JAMA Network Open. 2020; 3: e208759.

[2] Kitahara CM, Sosa JA. The changing incidence of thyroid cancer. Nature Reviews Endocrinology. 2016; 12: 646–653.

[3] Schneider DF, Chen H. New developments in the diagnosis and treatment of thyroid cancer. CA: A Cancer Journal for Clinicians. 2013; 63: 373–394.

[4] Abdullah MI, Junit SM, Ng KL, Jayapalan JJ, Karikalan B, Hashim OH. Papillary Thyroid Cancer: Genetic Alterations and Molecular Biomarker Investigations. International Journal of Medical Sciences. 2019; 16: 450–460.

[5] Yan T, Qiu W, Song J, Fan Y, Yang Z. ARHGAP36 regulates proliferation and migration in papillary thyroid carcinoma cells. Journal of Molecular Endocrinology. 2021; 66: 1–10.

[6] Cancer Genome Atlas Research Network. Integrated genomic characterization of papillary thyroid carcinoma. Cell. 2014; 159: 676–690.

[7] Gandolfi G, Ragazzi M, de Biase D, Visani M, Zanetti E, Torricelli F, *et al*. Genome-wide profiling identifies the THYT1 signature as a distinctive feature of widely metastatic Papillary Thyroid Carcinomas. Oncotarget. 2017; 9: 1813–1825.

[8] Chang S, Yim S, Park H. The cancer driver genes IDH1/2, JARID1C/KDM5C, and UTX/KDM6A: crosstalk between histone demethylation and hypoxic reprogramming in cancer metabolism. Experimental & Molecular Medicine. 2019; 51: 1–17.

[9] Sasanakietkul T, Murtha TD, Javid M, Korah R, Carling T. Epigenetic modifications in poorly differentiated and anaplastic thyroid cancer. Molecular and Cellular Endocrinology. 2018; 469: 23–37.

[10] Toska E, Osmanbeyoglu HU, Castel P, Chan C, Hendrickson RC, Elkabets M, *et al*. PI3K pathway regulates ER-dependent transcription in breast cancer through the epigenetic regulator KMT2D. Science. 2017; 355: 1324–1330.

[11] Li M, Shi M, Xu Y, Qiu J, Lv Q. Histone Methyltransferase KMT2D Regulates H3K4 Methylation and is Involved in the Pathogenesis of Ovarian Cancer. Cell Transplantation. 2021; 30: 9636897211027521.

[12] Augert A, Zhang Q, Bates B, Cui M, Wang X, Wildey G, *et al*. Small Cell Lung Cancer Exhibits Frequent Inactivating Mutations in the Histone Methyltransferase KMT2D/MLL2: CALGB 151111 (Alliance). Journal of Thoracic Oncology. 2017; 12: 704–713.

[13] Liang N, Niu Y, Ma T, Zhang X. 'Abstract 1639: Correlation of *KMT2C/D* loss-of-function mutations with PD-L1 expression and response to immune checkpoint inhibitors in solid tumors', AACR Annual Meeting 2021. Philadelphia, PA. 2021.

[14] Hillman RT, Celestino J, Terranova C, Beird HC, Gumbs C, Little L, *et al*. KMT2D/MLL2 inactivation is associated with recurrence in adult-type granulosa cell tumors of the ovary. Nature Communications. 2018; 9: 2496.

[15] Sun P, Wu T, Sun X, Cui Z, Zhang H, Xia Q, *et al*. KMT2D inhibits the growth and metastasis of bladder Cancer cells by maintaining the tumor suppressor genes. Biomedicine & Pharmacotherapy. 2019; 115: 108924.

[16] Maitituoheti M, Keung EZ, Tang M, Yan L, Alam H, Han G, *et al*. Enhancer Reprogramming Confers Dependence on Glycolysis and IGF Signaling in KMT2D Mutant Melanoma. Cell Reports. 2020; 33: 108293.

[17] Koutsioumpa M, Hatziapostolou M, Polytarchou C, Tolosa EJ, Almada LL, Mahurkar-Joshi S, *et al*. Lysine methyltransferase 2D regulates pancreatic carcinogenesis through metabolic reprogramming. Gut. 2019; 68: 1271–1286.

[18] Hou G, Xu W, Jin Y, Wu J, Pan Y, Zhou F. MiRNA-217 accelerates the proliferation and migration of bladder cancer via inhibiting KMT2D. Biochemical and Biophysical Research Communications. 2019; 519: 747–753.

[19] Li S, Jiang W, Xiao W, Li K, Zhang Y, Guo X, *et al*. KMT2D deficiency enhances the anti-cancer activity of L48H37 in pancreatic ductal adenocarcinoma. World Journal of Gastrointestinal Oncology. 2019; 11: 599–621.

[20] Froimchuk E, Jang Y, Ge K. Histone H3 lysine 4 methyltransferase KMT2D. Gene. 2017; 627: 337–342.

[21] Zhou C, Zhang Y, Dai J, Zhou M, Liu M, Wang Y, *et al*. Pygo2 functions as a prognostic factor for glioma due to its upregulation of H3K4me3 and promotion of MLL1/MLL2 complex recruitment. Scientific Reports. 2016; 6: 22066.